

Novel automatic off-resonance correction without field maps in spiral imaging using L1 minimization

Hisamoto Moriguchi¹, Kohki Yoshikawa², Morio Shimada², Shin-ichi Urayama³, Yutaka Imai¹, Manabu Honda⁴, and Takashi Hanakawa⁴

¹Radiology, Tokai University, Isehara, Kanagawa, Japan, ²Radiological Sciences, Komazawa University, Tokyo, Japan, ³Human Brain Research Center, Kyoto University, Kyoto, Japan, ⁴Functional Brain Research, National Center of Neurology and Psychiatry, Tokyo, Japan

Introduction: Spiral imaging has become popular due to its short scan time and its insensitivity to flow artifacts. A primary disadvantage of spiral imaging is blurring artifacts due to off-resonance effects. Most spiral off-resonance correction methods proposed to date require a frequency field map. The field map is usually obtained by taking phase difference between two spiral scans with slightly different TE's. Therefore, the total scan time is usually twice the time required for a single spiral acquisition. It would be desirable if off-resonance correction can be done without acquiring a field map for faster data acquisition. Automatic off-resonance correction methods without field maps have been proposed in previous literatures [1-4]. These methods estimate image phase from low frequency k-space data and determine the off-resonance frequencies based on the estimated phase. However, it is often difficult to determine the correct off-resonance frequencies using these methods in regions where high frequency data are dominant, e.g. rim and tissue boundaries. In this study, a novel spiral automatic off-resonance correction method that overcomes this difficulty has been demonstrated. In the newly proposed method, L1 minimization is used as a new criterion to determine the correct off-resonance frequencies in regions near edges of imaged objects. L1 minimization techniques have often been taken advantage of in compressed sensing [5]. It is well known that L1 minimization provides a sparse solution, i.e., the solution that consists of a few non-zero values and is otherwise zeros. On the other hand, if a spiral image is deblurred using the correct off-resonance frequency, edge definition is improved and thus spread signals due to off-resonance effects are focused into limited locations. The L1 min off-resonance correction proposed here capitalizes on this analogy. Frequency estimation process of the L1 min off-resonance correction is robust and the estimated field map shows reduced errors. The L1 min off-resonance correction has significant potential for faster spiral acquisition.

Methods: A flow chart of the L1 min off-resonance correction method is shown in Fig.1. In (a), a high pass filtered image is reconstructed to define the edges. This edge map is dilated after adequate thresholding to determine 'near-edge regions' where frequencies are to be estimated, as shown in (b). Frequency estimation will be done in the following steps: A stack of 'high-pass filtered images' are reconstructed using several different demodulation frequencies. The sum of absolute image values $\sum |I(x,y)|$ within a small window centered on each pixel is computed. These values are compared at the same location among all the frequency-demodulated images. The frequency that provides the lowest $\sum |I(x,y)|$ is selected as the correct off-resonance frequency. This estimation method is applied for the entire 'near-edge regions' defined in (b). A sample estimated field map is shown in (c). From this point on, frequencies in the rest regions of the image (referred to as 'far-edge regions') are to be determined. Since high spatial frequency components are not significant in these regions, a previously proposed automatic off-resonance correction method [1] is applied with a relative large window. However, since this method is intrinsically different from the L1 min method, there may be gaps for the estimated frequencies at the boundaries between near-edge and far-edge regions. To achieve smooth transition of the estimated frequencies at the boundaries, the following steps will be taken: Images corrected using the frequencies computed in (c) are inserted into the 'near-edge regions'. A low-pass filtered image is inserted into far-edge region. Based on the phase of this combined image (d), the previous correction method [1] is applied to the entire regions. Since a window located at the boundaries include both near-edge and far-edge regions, smoothly varying frequency can be computed as the window moves across the image while the frequencies estimated in near-edge regions in (c) are maintained. The final off-resonance correction is performed based on the field map.

MR experiment was performed to test the L1 min off-resonance correction using a 3.0 Tesla Siemens Trio Scanner. In this experiment, 20 interleaved spiral trajectories were designed with TE/TR/FA = 2.0/20.0ms/16°, readout time 14ms and FOV 270mm. Axial brain images were acquired from an asymptomatic volunteer. All procedures were done under an institutional review board approved protocol for volunteer scanning. The image matrix size was 256 x 256. In the L1 min off-resonance correction, the tested demodulation frequencies ranged from -200Hz to +200Hz with 10Hz interval. The size of small window to evaluate $\sum |I(x,y)|$ is 31 x 31 pixels. The same spiral sequence but with TE 4.0ms was also implemented to compute a field map from the phase difference between two images. A previous phased-based automatic correction method [2] was also implemented for comparison.

Results: Figure 2 shows field maps and reconstructed images: (a) the field map created using the proposed L1 min method, (b) the field map computed from the phase difference, (c) the field map created using the previous phase-based correction method, (d) off-resonance corrected image using the field map (a), and (e) the original image before correction. In (a)-(c), the frequencies from -80Hz to +80Hz are displayed and the gray values indicate the frequencies. As seen, (a) and (b) show quite similar tendency in frequency variations. (c) shows increased errors for regions near rim. As indicated by arrows and circles in (d), the definition of ventricles, brain rim and scalp are improved after off-resonance correction using the field map (a) when compared with (e).

Discussion and Conclusions: In the previously proposed automatic off-resonance correction methods [1-4], phase of deblurred image is estimated from the low-frequency k-space data since phase accrual due to off-resonance effects for central k-space data is not significant. However, this estimate does not provide accurate phase at rim and tissue boundaries of imaged objects because high-frequency components are dominant in these regions. The newly proposed L1 min correction method takes advantage of the fact that L1 value of spread signals are minimized when they are focused with correct demodulation. In our experiments, the L1 value $\sum |I(x,y)|$ on a high-pass filtered image has a single definite minimum of all the tested frequencies in most cases. Also, there is significantly low probability for the plot of $\sum |I(x,y)|$ vs. tested demodulation frequencies to have spurious minima for typical image contents. Therefore, the estimation process is stable for regions near rim and tissue boundaries. On the other hand, the previous methods have reduced errors in frequency estimation for the other regions of images. Using the procedures described in Fig1.(c)→(d), a smoothly varying field map can be created for the entire image. The newly proposed method eliminates need to acquire field maps and thus can achieve even faster spiral scan. Furthermore, this method is quite useful when acquired field maps are not so reliable, e.g. object motion is involved between two scans.

Acknowledgements: Siemens Healthcare. MEXT Grant-in-Aid for Scientific Research 22791223.

References: [1] Noll DC, et al. MRM 1992;25:319-333. [2] Man LC, et al. MRM 1997;37:906-913. [3] Chen W, et al. MRM 2006;56:457-462. [4] Chen W, et al. MRM 2008;59:1212-1219. [5] Candes EJ, et al. J Fourier Anal Appl 2008;14:877-905.

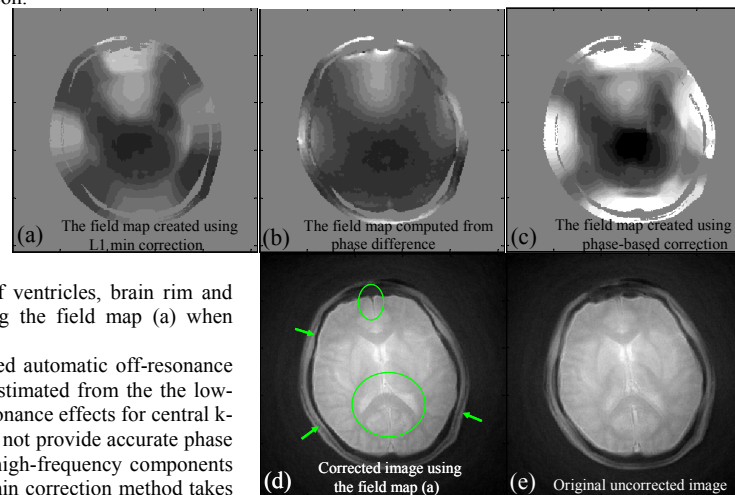


Fig.2. Field maps and reconstructed images

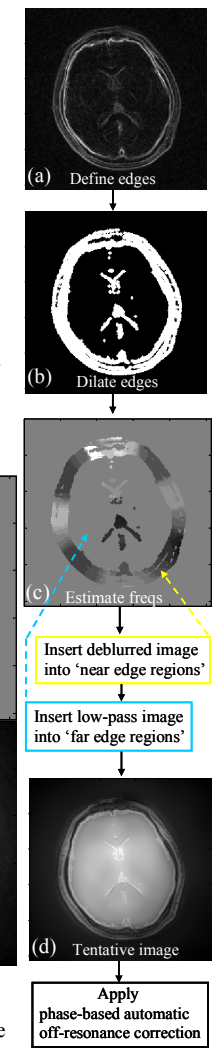


Fig.1. Flow chart of L1 min off-resonance correction